

Chapter 15

Astronomical and Geophysical Factors of the Perturbed Chandler Wobble of the Earth Pole



Sergej S. Krylov , Vadim V. Perepelkin , and Alexandra S. Filippova 

Abstract In the framework of the restricted three-body problem, a celestial–mechanical model of the steady-state Chandler wobble of the Earth pole is proposed. The contribution of the astronomical and geophysical disturbances to the observed Earth pole oscillations is discussed based on the processing of IERS observations of the Earth pole motion, NCEP/NCAR geophysical data of the atmospheric circulation, and NASA/JPL angular momentum of the ocean. The directions of the axes x' , y' corresponding to 50° of west longitude and 40° of east longitude, respectively, are found in the projection, onto which its coordinates have the maximum and minimum intensities of perturbed oscillations. The Earth pole oscillatory process that is in-phase with the lunar orbit precessional motion is studied, and the contribution of moving media to this process is discussed.

15.1 Introduction

The study of the fundamental astrometric problem of predicting the Earth pole motion [1] is of significant theoretical interest and fundamental for satellite navigation [2, 3]. One of its important problems is a high-precision forecast of the spacecraft orbits [4, 5]. In order to solve this problem, it is necessary to take into account various perturbing factors in the equations of motion [3, 6]. Accuracy improvement of the coordinate-time and navigation support of the satellite systems is closely related to the prediction of the Earth pole oscillations because, for example, the Earth orientation

S. S. Krylov · V. V. Perepelkin (✉) · A. S. Filippova
Moscow Aviation Institute (National Research University), 4, Volokolamskoe shosse, Moscow
125993, Russian Federation
e-mail: vadimkin1@yandex.ru

S. S. Krylov
e-mail: krylov@mai.ru

A. S. Filippova
e-mail: filippova.alex@gmail.com

parameters are included in the transformation matrix from the geocentric equatorial coordinate system to the Earth geographic coordinate system. One of the main problems in predicting the Earth pole motion is to take into account the parameters variability in the main components of the Earth pole oscillation (Chandler wobble and annual oscillatory process) [7].

Usually, the Chandler wobble is understood as the Earth pole oscillation with the frequency of free nutation of the Earth's rotation axis (with the Chandler frequency) in the Earth-bound coordinate system [8]. It can also be considered in a narrower sense, as a steady-state oscillation mode at the Chandler frequency and, in a broader sense, as a multi-frequency oscillatory process with a main frequency being close to Chandler's one. However, it is very difficult to give an unambiguous definition that would fully correspond to the physical process under consideration. Uncertainty in the interpretation of the Chandler component is due to the lack of a comprehensive explanation of the excitation mechanism. In some cases, it is convenient to use the terminology of the perturbation theory. If the steady-state regime of the Chandler wobble (with a constant frequency and average amplitude) is formally taken as an "unperturbed" motion, then the perturbations that lead to variations in the Chandler wobble parameters, which may be considered as perturbations, although it should be noted that the steady state of the Chandler wobble is also a perturbed motion.

Explaining the excitation mechanism of the Chandler wobble is one of the fundamental problems when studying the Earth pole motion. At least, a part of the perturbations leading to variations in the Chandler wobble parameters are caused by this mechanism. Therefore, the study of the variability of the main components parameters of the Earth pole oscillation (generally speaking, not only Chandler wobble, but also annual oscillations) is of considerable interest both for the task of predicting the Earth pole motion and the study of the excitation mechanism of the Chandler wobble. First of all, the problem is to identify the celestial-mechanical and geophysical reasons for such behavior of the Chandler component of the Earth pole oscillations.

Factors affecting the Earth motion relative to the center of mass can be divided into astronomical and geophysical. The Earth motion in space, as well as, the motion of the Earth's moving media occurs under the influence of the bodies in the solar system, and primarily under the Sun and the Moon. Therefore, when studying the Earth motion it is natural and necessary to take into account the astronomical and geophysical factors together. Lunar-solar gravitational perturbing forces lead to the precession and nutation of the Earth, the refined theory of which taking into account the internal structure of the Earth is in good agreement with observational data. In contrast to precession and nutation, the Earth deformability and the mobility of its various media are determining factors for the motion of the instantaneous axis of rotation in the Earth's body. And in this case, it is important to take into account not only the mobility of the media, but also the astronomical factors that influence them, since during the evolution of the solar system many processes must be considered as synchronized processes.

The purpose of this chapter is to study the oscillatory processes of the Earth pole under the perturbing astronomical and geophysical factors, as well as, the aspects of their synchronization. In Sect. 15.2, the definition of the unperturbed Earth pole

motion is introduced based on the celestial–mechanical model of the deformable Earth rotation. Tidal oscillations in the inertia tensor of a deformable Earth, which are taken into account in the framework of a simple celestial–mechanical model of its motion, are considered in Sect. 15.3. In Sect. 15.4, a correspondence between the intensity of perturbed oscillations in the Earth pole coordinates, the direction of the coordinate axes and the longitude distribution of the ocean surface is established based on the processing of astrometric and geophysical observation data. Section 15.5 is devoted to the study of the geophysical disturbances contribution to the synchronization between the Earth pole motion and precession of the lunar orbit. In Sect. 15.6, the main conclusions of the work are given.

15.2 Studying the Earth Rotation Within the Restricted Three-Body Problem

The study of the Earth motion relative to its center of mass under the lunar–solar gravitational–tidal and geophysical disturbances is based on the problem of a system consisting of a deformable planet (the Earth) and a point satellite (the Moon) moving around an attracting center (the Sun) [9–12]. The Earth and the Moon perform translational–rotational motion around the barycenter, which moves in orbit around the Sun (Fig. 15.1).

We introduce the inertial coordinate system $O\xi_1'\xi_2'\xi_3'$ with the origin in the attracting center O , where the axis $O\xi_3'$ is orthogonal to the orbital plane of the

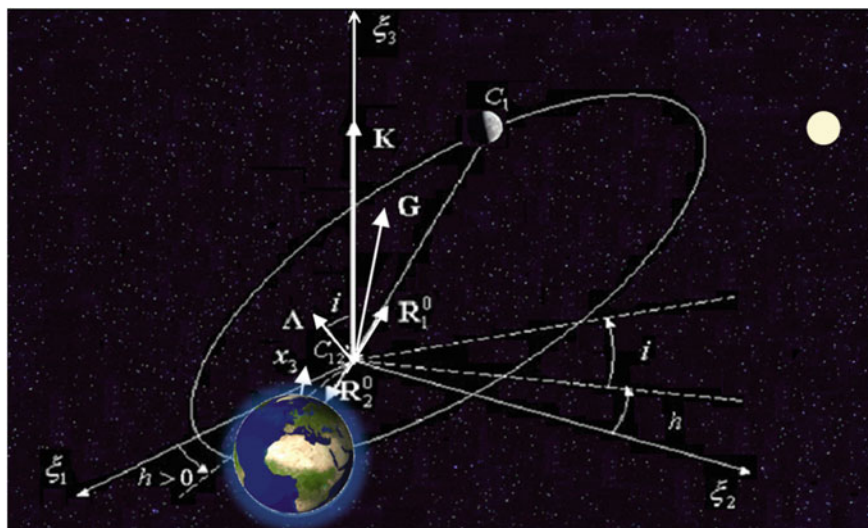


Fig. 15.1 Coordinate system for the two-body problem and orientation of the vectors

barycenter C_{12} , and the Koenig coordinate system $C_{12}\xi_1\xi_2\xi_3$. In an undeformed state, the Earth is dynamically compressed, i.e., $C > A$, where C and A are the axial and average equatorial moments of inertia, respectively. Let us bind the coordinate system $C'_2x_1x_2x_3$ with the deformable Earth, in a way that the axes are directed along the main central axes of the undeformed planet and the point C'_2 is the center of mass of the planet in the absence of deformations.

Let \mathbf{G} be the spin of the planet, $\mathbf{\Lambda}$ be the orbital angular momentum of the satellite's centers of mass C_1 and the planet's C_2 . In the absence of disturbances, the angular momentum of the system $\mathbf{K} = \mathbf{G} + \mathbf{\Lambda}$ is stationary in inertial space and coincides with the $C_{12}\xi_3$ axis (Fig. 15.1).

The deformable Earth motion relative to the center of mass can be described in the canonical variables of Andoyer (Fig. 15.2) $L, G, G_{\xi_3}, \varphi_1, \varphi_2, \varphi_3$, ($G = |\mathbf{G}|$, L is a projection of the vector \mathbf{G} on the axis C'_2x_3 , and G_{ξ_3} is a projection of the vector \mathbf{G} on the $C_{12}\xi_3$). We describe the mutual orbital motion of the centers of masses C_1 and C_2 in the Delaunay canonical variables Λ, H, ϑ, h ($\Lambda = |\mathbf{\Lambda}|$, H is the projection of the vector $\mathbf{\Lambda}$ on the $C_{12}\xi_3$ axis, ϑ is the mean anomaly, and h is the longitude of the ascending node of the orbit on the $C_{12}\xi_1\xi_2$ plane).

In the bounded coordinate system, the unit vectors \mathbf{R}^0_{21} and \mathbf{R}^0 , which specify the directions from the Earth to the Moon and from the Sun to the barycenter, respectively, are defined as follows equations:

$$\begin{aligned} O^{-1}(t)\mathbf{R}^0_{21} &= (\gamma_1, \gamma_2, \gamma_3)^T, \\ O^{-1}\mathbf{R}^0 &= (\kappa_1, \kappa_2, \kappa_3)^T. \end{aligned}$$

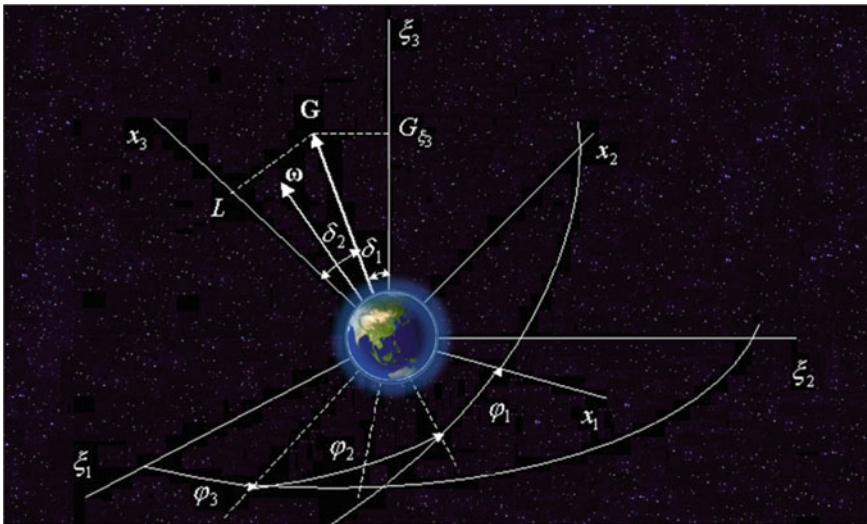


Fig. 15.2 Mutual orientation associated with the deformable Earth and reference coordinate systems in Andoyer variables

For practical applications, the transformation between two geocentric coordinate systems is important—the König one $C_2\xi_1\xi_2\xi_3$ and the Earth-bound one $C_2x_1x_2x_3$. This conversion is carried out by five consecutive rotations at the angles $\varphi_1, \delta_2, \varphi_2, \delta_1, \varphi_3$ according to Eq. 15.1.

$$O^{-1}(t) = \Gamma_3^{-1}(\varphi_1)\Gamma_1^{-1}(\delta_2)\Gamma_3^{-1}(\varphi_2)\Gamma_1^{-1}(\delta_1)\Gamma_3^{-1}(\varphi_3) \quad (15.1)$$

The matrix $O(t)$, which defines the transition from the Earth-bound to inertial axes, is expressed in canonical Andoyer variables, and $\cos \delta_1 = G_{\xi_3}/G$, $\cos \delta_2 = L/G$, (Fig. 15.2). The last two angles δ_1 and φ_3 in transformation (Eq. 15.1) are determined by the precession and nutation of the Earth and for this study are considered known and given. The angles φ_1 and δ_2 are the polar coordinates of the Earth pole and the variations of the angle φ_2 , which are associated with the irregularities of the Earth rotation, lead to variations of Universal Time UT1 [1].

The values of the pole shift and variations of Universal Time are very small: they do not exceed $0.5''$ for the annual Earth pole motion and 0.03 s for the annual amplitude of Universal Time variations. Changes in the angles of $\varphi_1, \delta_2, \varphi_2$ are significantly affected by the Earth deformations. The determination of variations in the inertia tensor of the deformable Earth is necessary to calculate the vector of the angular momentum, as well as, its total derivative by time, which is used to study both the perturbed and unperturbed Earth motion relative to its center of mass.

The most convenient generalized coordinates to qualitative describe the Earth's rotation around its center of mass are the canonical action-angle variables. The variables $I_1 = L, I_2 = G, I_3 = G_{\xi_3}, \varphi_1, \varphi_2, \varphi_3$ are the action-angle variables in the dynamically symmetrical Earth case.

For a qualitative description of the Earth motion relative to its center of mass, when taking into account the impact of disturbances from the Moon and the Sun, the linear theory of viscoelasticity of small deformations is used. The perturbed Routh functional of the problem under consideration can be represented in the form of Eq. 15.2 [9].

$$R = R_0 + \varepsilon R_1(\{I\}, \{\varphi\}, [\mathbf{u}], [\dot{\mathbf{u}}]) + \varepsilon^2 \dots \quad (15.2)$$

Here, R_0 is the Routh functional in the absence of deformations including the functionals of the system's kinetic energy and potential energy of gravitational forces from the Moon and the Sun, εR_1 is the perturbation functional due to gravitational tides that includes the kinetic energy of the relative motions of the elastic body particles and potential energy of elastic deformations, $\mathbf{u}, \dot{\mathbf{u}}$ are vectors of displacement and velocity of the moving medium particles; $\varepsilon > 0$ is a small dimensionless parameter characterizing the relative magnitude of the perturbing factors in Eq. 15.2, which is introduced for convenience.

The dynamics of the perturbed Chandler motion of the instantaneous axis is related, in particular, with a change in the angle δ_2 , which determines the change in the amplitude of the Chandler wobble. The angular variable δ_2 is the angle between the axis of the figure of the Earth and the vector of the Earth's spin.

In the absence of dynamic symmetry ($A \neq B$), the action-angle variables will differ from the Andoyer variables by small changing values, and the desired equations taking into account the perturbed functional εR_1 will take the form of Eqs. 15.3, where h_1 is the integral of the kinetic energy for the unperturbed problem.

$$\begin{aligned} \dot{I}_1 &= -\varepsilon \frac{\partial R_1}{\partial w_1} & \dot{I}_2 &= 0 & \dot{I}_3 &= -\varepsilon \frac{\partial R_1}{\partial w_3} \\ \dot{w}_1 &= n_1 + \varepsilon \frac{\partial R_1}{\partial I_1} & \dot{w}_2 &= n_2 + \varepsilon \frac{\partial R_1}{\partial I_2} \\ \dot{\delta}_2 &= -\varepsilon (I_2 \kappa_* \sin \delta_2)^{-1} \frac{1 + \kappa^2 \sin^2(\eta, \lambda)}{\text{dn}(\eta, \lambda)} \frac{\partial R_1}{\partial w_1} \\ \eta &= \frac{2}{\pi} \mathbf{K}(\lambda) w_1 & \kappa^2 &= \frac{C(A-B)}{A(B-C)} & \lambda^2 &= \kappa^2 \frac{2Ch_1 - I_2^2}{(I_2^2 - 2h_1 A)} \end{aligned} \quad (15.3)$$

The model of the Chandler pole motion with the frequency $\dot{w}_1 = n_1$ and identification of its parameters are based on the qualitative theory of dissipative systems. To determine the steady pole motion as an unperturbed motion, the dissipative terms of the pole tide are taken into account in the variations of the centrifugal moments of inertia δJ_{pr} , δJ_{qr} . To do this, the Routh functional \mathcal{R}_{01} of the perturbed problem is introduced as Eq. 15.4.

$$\mathcal{R}_{01} = -L\sqrt{G^2 - L^2} \left(\frac{\delta J_{\text{pr}} \sin l}{A C} + \frac{\delta J_{\text{qr}} \cos l}{B C} \right) \quad (15.4)$$

Variations in the centrifugal moments of inertia due to variable rotational deformation are associated with variations in the tesseral harmonics of the geopotential with simple relations [10]. The amplitudes of the variable normalized tesseral harmonic coefficients $\delta \bar{c}_{21}$, $\delta \bar{s}_{21}$ are determined from geophysical measurements and, according to [1], are related to the coordinates of the Earth pole by the relations:

$$\begin{bmatrix} \delta \bar{c}_{21} \\ \delta \bar{s}_{21} \end{bmatrix} = -1.33 \cdot 10^{-9} \left(\begin{bmatrix} x_p \\ y_p \end{bmatrix} + 0.0115 \begin{bmatrix} y_p \\ -x_p \end{bmatrix} \right).$$

Taking these terms into account, Eq. 15.4 leads to the damping of the pole motion at a frequency of n_1 .

The perturbed motion taking into account the dissipative properties of the Earth viscoelastic mantle leads to regular precession with slowly changing parameters, which can be studied on the basis of asymptotic methods of nonlinear mechanics [11, 12]. And, in particular, the steady state of the Chandler wobble is determined.

When considering the perturbed case for \mathcal{R}_{01} taking into account the dissipative terms of the pole tide in the variations of the centrifugal moments of inertia, as well as, the small perturbation at the Chandler frequency n_1 in a form of

$$\begin{aligned} \frac{\delta J_{\text{pr}}}{A^*} &= -\sigma \delta_2 \sin w_1 + \mu_p \cos(n_1 t + \beta_p), \\ \frac{\delta J_{\text{qr}}}{B^*} &= -\sigma \delta_2 \cos w_1 + \mu_q \cos(n_1 t + \beta_q), \end{aligned} \quad (15.5)$$

we obtain Eq. 15.6 for coefficient δ_2 .

$$\dot{\delta}_2 \approx -\frac{2r_0 K(\lambda)\kappa}{\pi\chi} \sigma \delta_2 + f_p \sqrt{1+\kappa^2} \sin w_1 \cos(Nt + \beta_p) + f_q \cos w_1 \sin(Nt + \beta_q) \quad (15.6)$$

Here, σ is the dissipation coefficient, $f_{p,q}$ and $\beta_{p,q}$ are the amplitudes and phases of the perturbation, respectively.

In stationary steady state, we will have Eq. 15.7.

$$\delta_2 \approx \frac{f_q \sin(\beta_q + \Delta\psi) + f_p \sqrt{1+\kappa^2} \cos(\beta_p + \Delta\psi)}{4r_0 K(\lambda)\kappa\sigma(\pi\chi)^{-1}} \quad (15.7)$$

$$f_q \cos(\beta_q + \Delta\psi) - f_p \sin(\beta_p + \Delta\psi) = 0$$

To study the dynamics of the Earth pole motion, the steady-state mode of its oscillations can be taken as unperturbed. Factors that perturb the steady motion of the Earth pole are astronomical (lunar–solar disturbances) and geophysical ones. The obtained model of the Earth pole unperturbed oscillatory process is also convenient for constructing a numerical–analytical model for predicting its motion [13].

15.3 Tidal Oscillations of the Deformable Earth Inertia Tensor

Modern methods of gravimetry, geophysics, and space geodesy make it possible to measure with high accuracy the temporal variations of the geopotential expansion coefficients and the corresponding small radial vibrations of the Earth's surface. These fluctuations occur mainly due to the lunar–solar tidal disturbances and geophysical phenomena. For example, the amplitudes of solid-state tides from the Moon and the Sun measured on the Earth's surface reach 34 and 16 cm, respectively. The magnitudes of these amplitudes are in accordance with the magnitudes of the equipotential surface oscillation amplitudes of the tidal potential and, to a first approximation, are connected by a linear dependence. The proportionality coefficient between the surface level heights of the tidal potential and the Earth's surface is determined from observations. It is associated with many physical and mechanical characteristics of the deformed Earth. The lunar–solar tidal potential leading to terrestrial tides—solid, oceanic, and atmospheric—also turns out to be proportional to the corresponding changes in geopotential. The estimate value of these proportionality coefficients depending on the parameters of the planet's deformations—elastic moduli and viscosity coefficients of various media, as well as, the disturbance frequency—makes it possible to solve the complex problem of studying the Earth's internal structure. This line of research is a branch of geophysics. But the problem of the deformable Earth motion relative to its center of mass is a complex task and can combine elements of various fields of science: astrometry, celestial mechanics,

geophysics, the theory of stochastic systems, and many others. And first of all, the methods and approaches used to construct the Earth motion model depend on the goals of scientific research. In that case, if the goal of the problem is modeling in a certain “average” sense that is a development of a model described the motion in question with average observed parameters, then the celestial–mechanical approach seems to be the most rational as the basis for constructing a complex model. Along with this, it is justified from the point of view of practical application to construct a few-parameter mathematical forecast model that allows us to reduce the computational complexity of the algorithmic implementation of the model of the Earth orientation parameters oscillations.

Indeed, for qualitative conclusions about the Earth motion around its center of mass, it will be logically justified to take into account coherent oscillations in various deformable (visco-elastic and liquid) Earth’s media. For example, Fig. 15.3a shows the observed oscillations of the gravitational acceleration normal component δg on an SG gravimeter in Membach (Belgium), whose position is marked on the static

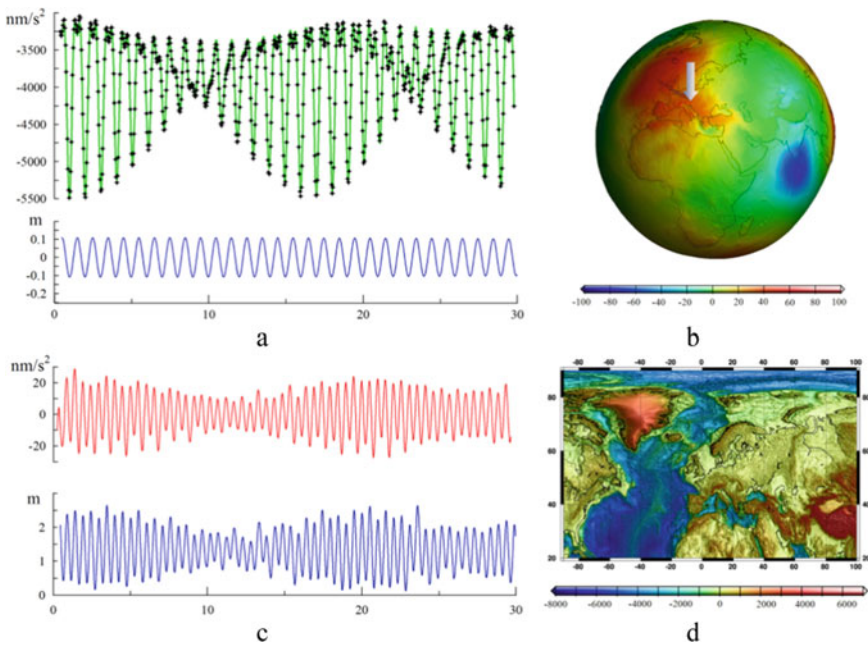


Fig. 15.3 Earth motion observation: **a** variations in the gravitational acceleration according to measurements on an SG gravimeter in Membach (discrete points) in comparison with fluctuations in the model of solid-state tides (green line) and diurnal variations in sea level according to PSMSL station near Rorvik, **b** model of the geoid of the GFZ center (the arrow shows the location of the city of Membach), **c** comparison of hydrosphere tidal oscillations in the data of the gravitational acceleration of the Membach city (red line) and sea-level fluctuations in the Rorvik city (blue line), and **d** geoid elevation map for a portion of the Earth’s surface according to the model of the GFZ center (the flag marks the location of Rorvik)

geoid of the GFZ model [14]. An example of comparing the δg variations due to solid-state tides with the measurement data shows that the combined tidal variations of the Earth's deformable media determine 98% of the observed oscillations. These coherent fluctuations in geomeia can be identified with the ones of a viscoelastic thin layer of the adopted deformable Earth model. Then the differences between the solution of such a model problem obtained in the first approximation and observed processes will be in the proportionality coefficients. In turn, these coefficients can be identified with a sufficient degree of accuracy from astrometric and geodetic observations and measurements data. This approach allows some generalization in the case of taking into account hydrosphere oscillations. Indeed, if the oceanic oscillations are taken into account, we can assume that the remaining discrepancy in the oscillations of the measured signal δg along with the influence of atmospheric pressure [15] will also be caused by hydrosphere fluctuations from a relatively small (on the scale of the entire Earth's surface) neighborhood. Variations in atmospheric pressure are usually non-stationary and measured directly at the point of observation. The corresponding fluctuations in the gravitational acceleration can be considered proportional to atmospheric pressure [15, 16]: they can be easily filtered out. However, atmospheric fluctuations in the high-frequency range like any tidal variations of the atmosphere are small. Therefore, the remaining 2% of the amplitude of the high-frequency g oscillations will be due to hydrosphere fluctuations. As an example of the correlation between the variations in the gravitational acceleration and local hydrosphere, a comparison is made (Fig. 15.3b) between the sea-level fluctuations at the coastline of Rorvik (Norway) marked on the map without the long-period component and the corresponding component isolated from δg . Also, in Fig. 15.3a, the gravitational accelerations and close to diurnal sea level variations are compared. For example, if the residual between the measurement data and tidal model of the solid-state oscillations of the gravitational acceleration is represented as the sum of the diurnal and semidiurnal variations $\delta g^\varphi + \delta g^{2\varphi}$, then it correlates with the variation $\delta h^\varphi - \delta h^{2\varphi}$ of the sea level.

15.4 Geophysical Factors in the Model of the Earth Pole Oscillatory Process

It is well-known [1, 17, 18] that the amplitude and phase of the Chandler component of the Earth pole oscillatory process are very sensitive to various perturbing factors including those with irregular properties (oceanic, atmospheric, and possibly others). The magnitude of the amplitude of the steady-state motion is determined by the frequency difference and dissipation coefficient. Therefore, the Chandler component of the Earth pole oscillations should be considered the most sensitive to the irregular impacts. The mechanism of these impacts is naturally related to weak inertia tensor perturbations.

Even the regular tidal potential [16], due to the complexity of the topography of the global ocean floor and contours of the continents coastlines, leads to the development of a random displacement field and occurrence of random fluctuations in tidal processes. These perturbations correspond to weak irregular perturbations of the Earth’s inertia tensor components. However, due to the uneven distribution of the global ocean’s water masses over the Earth’s surface, their manifestation in the centrifugal moments of inertia J_{xz} , J_{yz} , and, therefore, in the coordinates x_p , y_p , are different.

In Fig. 15.4, the amplitude spectrum of the Earth pole coordinates in the axes x , y (left graph) and x' , y' (right graph) are shown. The axes x , y correspond to the terrestrial coordinate system ITRS axes [1] (the axis x is located in the Greenwich meridian plane, and axis y is in the plane orthogonal to it). In turn, axes x' , y' are obtained by rotating x , y by an angle determined from the fulfillment of the combined condition of the noise’s highest level (the level of the spectral power density of the

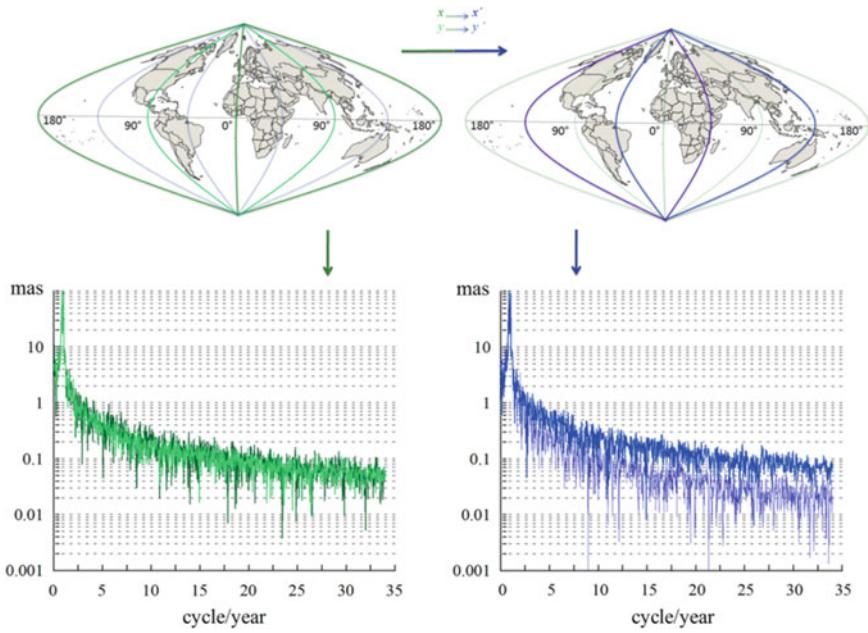


Fig. 15.4 Amplitude spectrum of the Earth pole coordinates. At the bottom left, we see the amplitude spectra of the oscillations of the Earth pole coordinates in the projection on the axis x , y (dark green and light green lines, respectively). At the bottom right, we see the amplitude spectra of oscillations of the Earth pole coordinates in the projection on the axis x' , y' (dark blue and blue lines). The upper figure illustrates a relative position of the axes x , y (dark green and light green lines) corresponding to the zero meridian and the 90th meridian of west longitude (top left) and the axes x' , y' (dark blue and blue lines, respectively) obtained by turning the first two at an angle of 40° toward the east (top right). The logarithmic scale for amplitudes was used along the ordinate axis of the spectral graphs. The graphs show differences in the harmonics amplitudes of the high-frequency regions along the corresponding axes before and after the rotation

oscillations of the Earth pole coordinates x'_p, y'_p) in one of the coordinates and the lowest level in the other. The calculations were carried out in a 5° increment.

The resulted graphs show the differences in the harmonics amplitudes of the high-frequency regions. The logarithmic scale for amplitudes was used along the ordinate axis of the graphs. The graphs show that the lowest level of noise (in the frequency range from 5 to 40 cycles per year) is observed at the coordinate x' , rotated by an angle of about 40° to the east of Greenwich. The highest level of high-frequency oscillations approximately corresponds to the y' axis, which preserves the direction orthogonal to the x' axis, although the maximum is less explicit than the minimum along the x' axis.

The correspondence of the positions of the axes x', y' to the distribution of water mass over the Earth's surface can be shown visually using simple reasoning. First, we determine the dependence of the total ocean surface ratio to the land surface on longitude. To obtain accurate results, topographic data should be used, followed by their integration over latitude. However, since a high accuracy is not required for a qualitative analysis, we can consider a more original method, which is quite suitable for the purposes of this work. In [19], the results of broadband photometry of the Earth were presented according to the data from the Deep Impact spacecraft operating under the EPOXI mission, and the dependence of the land surface distribution on the longitude was constructed on the basis of light curves. Denote by $k(\theta)$ the share of the ocean surface at longitude θ is defined by Eq. 15.8.

$$k(\theta) = \frac{\text{Ocean Surface at longitude } \theta}{\text{Earth Surface at longitude } \theta} \quad (15.8)$$

Variations in the centrifugal moments of inertia $J_{x'z}, J_{y'z}$ have a perturbing effect on the Earth pole oscillatory process. Since the centrifugal moments of inertia characterize the masses distribution relative to the coordinate planes $x'z, y'z$, their sensitivity is higher to the motion of the moving medium on the Earth's surface that is located closer to the corresponding plane. Then they will have the greatest sensitivity to tangential displacements in a sector bounded by two meridians and containing a plane with respect to which the moments of inertia are calculated. In this case, the motion of particles on the surface bounded by such a sector occurs in tangential directions, but their latitude is unknown, since the introduced coefficient $k(\theta)$ as an integral value does not depend on latitude and there is no resolution on latitude.

Now we choose two sectors that are symmetrical with respect to the coordinate planes $x'z, y'z$ with angles at the vertex $2\theta_0$. When the axes are rotated, the selected sectors will also rotate. If the moving medium is evenly distributed over the surface of the hemisphere (e.g., for $x' > 0$) and is "frozen" on the opposite hemisphere, then the particle motion on the surface bounded by such a sector determine approximately $100 \sin \theta_0\%$ of the variable part for the centrifugal moments of inertia (at $\theta_0 = \pi/2$ the sector becomes a hemisphere). For an unevenly distributed medium, this value can differ and the smaller the angle $\theta_0 \in (0, \pi/2]$, the larger the difference. But on the other hand, the larger the angle θ_0 (i.e., the larger the area of the surface under consideration), the greater the uncertainty of the correspondence between the ocean

distribution and the total coefficient $k(\theta)$ in the sector after integration over longitude is. Therefore, the choice of the sector's angle (basically, the choice of the integration region of the coefficient $k(\theta)$ in longitude) is a compromise between the maximum sensitivity of centrifugal moments of inertia to the particles motion along a surface that is limited by the sector and the minimum area of this surface in order to reduce the uncertainty error. Since the share of the surface area limited by a sector is $2\theta_0/\pi$, θ_0 is determined from the condition that the function $\pi \sin \theta_0 - 2 \theta_0$ is maximum on the $0 < \theta_0 \leq \pi/2$ interval. Under the condition $\theta_0 \approx 0.9$, the motion of the particles in this sector determines approximately 80% variations of the tesseral harmonic of the geopotential. However, let us choose a slightly larger value of the angle and, in the following formulas, put for illustration purposes $\theta_0 = \pi/3$, although this will not fundamentally affect the estimates of average values.

Let us determine the share of the ocean surface area limited by one selected sector. Since the Earth's surface area limited by a sector is a constant and does not depend on the Earth rotation, the share of the ocean's surface area in the sector with an vertex angle as $(\theta - \pi/3, \theta + \pi/3)$ is proportional to the average coefficient $k(\theta)$:

$$\bar{k}(\theta) = \langle k(\theta) \rangle_{2\pi/3} = \frac{3}{2\pi} \int_{\theta-\pi/3}^{\theta+\pi/3} k(\theta) d\theta. \quad (15.9)$$

The centrifugal moments of inertia $J_{x'z}$, $J_{y'z}$ are most sensitive to the motion of the moving medium if the ocean distributions in the selected sector and in the sector symmetrical to it are significantly different. This condition can be replaced in a non-strict sense by the integral condition $\bar{k}(\theta) - \bar{k}(\theta + \pi) \neq 0$. In the strict sense, this condition does not appear directly from Eq. 15.9 and thus is taken as an assumption. If the location of the axes x' , y' meets this condition, then the assumption will be valid.

In order to establish a correspondence, a function is defined

$$f(\theta) = [\bar{k}(\theta) - \bar{k}(\theta + \pi)]^2 \quad (15.10)$$

that when $\bar{k}(\theta) = \bar{k}(\theta + \pi)$ takes the minimum value, i.e., with equal share of the ocean surface in two opposite sectors, and the maxima corresponds to the extrema of the function $\bar{k}(\theta) - \bar{k}(\theta + \pi)$, when the share of the ocean surface in two opposite sectors are most different.

The correspondence between the location of the axes x' , y' and the distribution of the ocean over the Earth's surface is shown in Fig. 15.5. It can be seen that the directions of the axes approximately correspond to the extrema of the function $f(\theta)$.

That is, in the approximately orthogonal direction to the axis x' one can assume a minimum of the amplitude of high-frequency perturbations due to less asymmetry in the ocean distribution, which, according to the results of processing the pole motion data, leads to high-frequency oscillations along the coordinate x' with lower intensity. Similarly, with respect to the coordinate y' , the oscillations with a higher

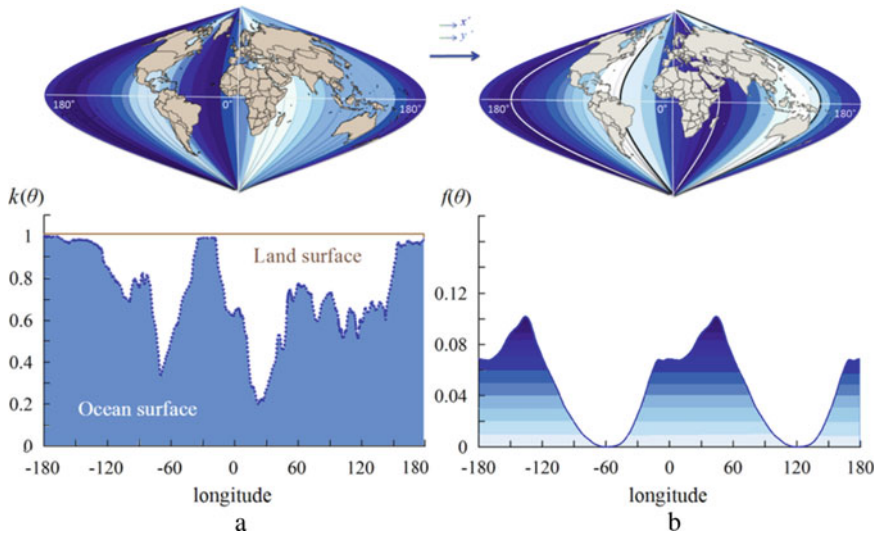


Fig. 15.5 Real and estimated distributions: **a** distribution of the ocean (blue color) and land (white color) on the Earth's surface depending on longitude (top) and share of the ocean surface at longitude θ (bottom), **b** distribution of the function $f(\theta)$ plotted on the Earth's map and the location of the axes x', y' corresponding to Fig. 15.4 (top) and dependence of the function $f(\theta)$ and the correspondence of its extrema to the location of the axes x', y' (bottom)

intensity are observed due to the greater asymmetry of the ocean distribution along the axis x' . Although it does not follow directly from the maximum in the axis y' and the minimum in the axis x' of the short-period pole oscillations that the intensity of the high-frequency perturbation in the projection onto the axis x' exceeds the intensity of the perturbation in the projection onto the axes y' , and not, for example, vice versa. Moreover, the maximum and minimum amplitudes of high-frequency perturbations can be achieved also while projecting on non-orthogonal axes. But from the analysis of the calculated total geodetic perturbations and separately the ocean perturbations in the projection on the axes x', y' , it can be established that the highest intensity of high-frequency perturbations is observed in the projection on the axis of approximately 15° of the east longitude and the lowest intensity is about 75° of the west longitude. These directions differ from the directions of the axes x', y' in the projection onto which the extrema of the amplitudes of the short-period Earth pole oscillations are observed, but with the same error correspond to the extrema of the function $f(\theta)$. Of course, for more accurate conclusions, it is important not only to estimate the asymmetry in the distribution of various media over the surface, but also to quantify the distributions, as well as, the latitude distribution. However, the calculations performed allow us to draw some conclusions.

Thus, the orientation of the vector of complete geodesic perturbations including the influence of the atmosphere and the ocean corresponds to the distribution of the ocean over the Earth's surface in the sense considered above. Consequently,

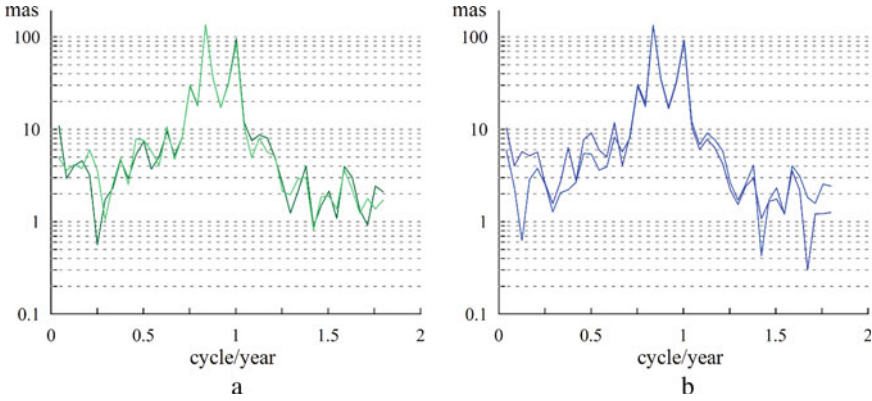


Fig. 15.6 Amplitude spectra of the oscillations of the Earth pole coordinates in the projection: **a** on the axis x, y (dark green and light green lines, respectively), **b** on the axis x', y' (dark blue and blue lines, respectively)

geophysical perturbations are some consistent oscillations of moving media and can be considered together as a combination.

The directions of the axes x', y' found from the condition of maximum and minimum intensities of perturbations approximately correspond to the distribution of the ocean over the Earth's surface, not only for high-frequency oscillations, but also for oscillations from any not too short frequency interval. That is, the correspondence can be shown for the entire spectrum of oscillations with the only caveat that for perturbations with frequencies below the Chandler frequency the arrangement of the axes x', y' , it will change by 90° . This means that the maximum amplitude of the pole oscillations at a frequency above the Chandler's one will be observed along the axis y' , and the maximum amplitude at a frequency below the Chandler's one will be observed along the axis x' (Fig. 15.6). This circumstance is also due to the correspondence of the phases with the fluctuations spectrum onto which the perturbations are decomposed. And this also indicates the consistency of perturbations of various physical nature.

15.5 The Role of Astronomical Factors in the Perturbed Earth Pole Motion

It is known [20] that coherent oscillations in various media can appear in the geophysical processes on a planetary scale. A number of large-scale phenomena of the atmosphere and the ocean, the global seismic activity of the Earth have signs of common oscillatory processes also inherent in the Earth rotational motion [21–23]. And the Chandler wobble is no exception. However, the process of developing such oscillations has not been sufficiently studied to this moment. For example, the variations

in the main components parameters of the Earth pole oscillations may have more global causes than it is assumed, and the process of their excitation is caused not only by fluctuations of geophysical media of a stochastic nature. More precisely, these oscillations can be non-stationary, but be of a natural nature, and not stochastic. From the result of processing data on the Earth pole motion, it appears [18] that the oscillations of the Earth's moving media in the spectral range of the Chandler and annual harmonics turn out to be ordered in some way. For example, in the observed Earth pole motion, it is possible to establish the presence of an in-phase oscillatory process with a precession of the lunar orbit [9, 18].

The spatial motion of the lunar orbit consists of a series of rotations around intersecting axes. They lead to the cyclical motion of its nodes and perigee [24]. In addition, the derivatives of the orbit parameters are nonzero and are varying values, being the subject to small variations. A result of the lunar orbit precession and of the associated cyclic change in the longitude of the ascending node with a period of 18.61 years is a change in the orbit plane inclination to the Earth's equator. The inclination of the lunar orbit to the Earth's equator varies from 18.3° to 28.58° . In this case, the point of intersection of the lunar orbit circle with the equator oscillates along the equator near its average position, which coincides with the point of the vernal equinox. Unlike the node (the intersection point of the lunar orbit circles and the ecliptic in the celestial sphere), which makes a complete revolution, the intersection point of the orbit and the equator oscillates in the range from -13.2° to 13.2° .

In [25], it was shown that one can find a transformation of the Earth pole coordinates, illustrating in-phase nature of its Earth pole oscillatory process and the lunar orbit precession. Namely, the oscillatory motion of the pole minus the Chandler (or annual depending on the amplitudes values of the Chandler and annual harmonics) and six-year cycles occurs in-phase with oscillations along the equator of the intersection point of the lunar orbit and the equator. This feature requires a more detailed analysis and study of the causes of such fluctuations. In particular, it is of interest to establish the contribution of geophysical (atmospheric and oceanic) disturbances to these oscillations.

As a result of the numerical solution of the differential equations of the Earth pole motion, the trajectories of the pole are obtained for various perturbations. The perturbing functions were tabulated according to the IERS published data. For example, in Fig. 15.7, it is shown a comparison between the fluctuations in the calculated motion of the Earth pole taking into account the combined perturbations from the atmosphere and the ocean and the fluctuations of its observed motion.

To isolate the oscillatory process with a frequency of 0.05373 cycle/year from the calculated and observed pole oscillations, the procedure proposed in [25] was applied. Using transformations of the Earth pole coordinates, the essence of which is the elimination of two cycles—with the Chandler and six-year periods, it is possible to obtain a pole oscillation in-phase with the precession of the lunar orbit. In Fig. 15.8a, a comparison is shown between the variations of the polar angle φ isolated from the observed Earth pole trajectory, its approximation by a two-frequency model with constant coefficients, and the calculated Earth pole trajectory taking into account atmospheric and oceanic perturbations. In the lower graph of Fig. 15.8, a graph of

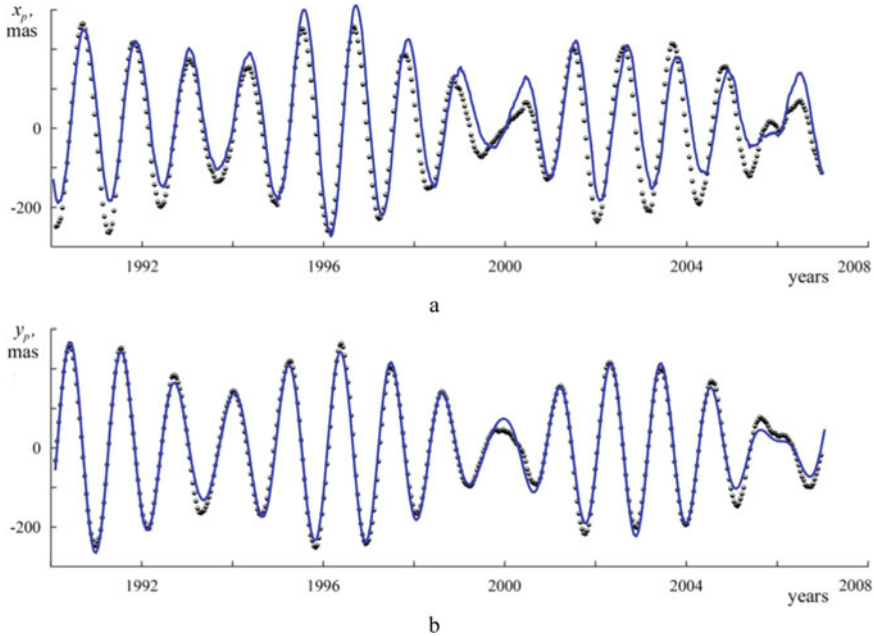


Fig. 15.7 Earth pole oscillations according to the IERS observations and measurements (discrete data) in comparison with the calculated oscillations caused by perturbations of: **a** atmosphere and **b** ocean

oscillations of the angle of deviation δ along the equator of the point of intersection of the equator with the lunar orbit is constructed. The main harmonic with the precession frequency of the lunar orbit for the observed pole motion is shown by the red line, and the blue dots are for the calculated motion taking into account geophysical perturbations. The oscillations caused by geophysical perturbations have much smaller amplitude and shifted phase, which indicate more complex physical nature of these oscillations and the incompleteness of the disturbances taken into account.

15.6 Conclusions

Variations in the main components parameters of the Earth pole motion are due to the effect of the combined nature. The considered main geophysical perturbations are apparently part of the coherent oscillations of various media. Not more than 50% of the energy of the considered oscillatory process is due to perturbations of the atmosphere and the ocean. Since the impact of other geophysical fluids on the Earth pole motion is much smaller, this process should be more global in nature and such variations in the Earth's environment can be affected. Then, their excitation

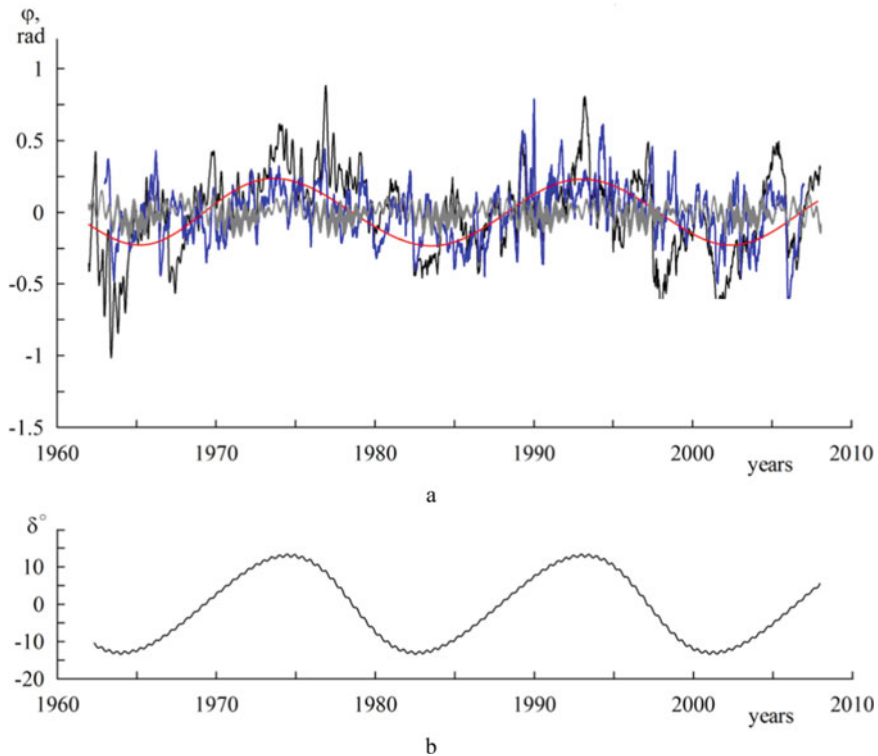


Fig. 15.8 Estimates of the polar angle variations: **a** comparison between the variations of the polar angle φ isolated from the observed Earth pole trajectory (black line), its approximation (red line), variations of the polar angle φ using a two-frequency model with constant coefficients (gray line), and the calculated Earth pole trajectory taking into account the atmospheric and oceanic perturbations (blue line) and **b** a graph of oscillations of the deviation angle δ along the equator of the point of intersection of the equator with the lunar orbit

in geomedia can be caused not so much by internal perturbations as by external disturbances for the Earth.

Acknowledgements This work was carried out within the basic part of the state task of the Ministry of Education and Science of the Russian Federation (project no. 721).

References

1. International Earth rotation and reference systems service—IERS annual reports, <https://www.iers.org>. Last accessed 9 Sept 2020
2. Markov, Y.G., Mikhaylov, M.V., Lar'kov, I.I., Rozhkov, S.N., Krylov, S.S., Perepelkin, V.V., Pochukaev, V.N.: Fundamental components of the parameters of the Earth's rotation in forming

- high-precision satellite navigation. *Cosmic Res.* **53**, 143–154 (2015)
3. Markov, Y.G., Mikhailov, M.V., Perepelkin, V.V., Pochukaev, V.N., Rozhkov, S.N., Semenov, A.S.: Analysis of the effect of various disturbing factors on high-precision forecasts of spacecraft orbits. *Cosmic Res.* **54**, 155–163 (2016)
 4. Petukhov, V.G.: Application of the angular independent variable and its regularizing transformation in the problems of optimizing low-thrust trajectories. *Cosmic Res.* **57**, 351–363 (2019)
 5. Ivanyukhin, A.V., Petukhov, V.G.: Low-energy sub-optimal low-thrust trajectories to libration points and halo-orbits. *Cosmic Res.* **57**, 378–388 (2019)
 6. Starchenko, A.E.: Trajectory optimization of a low-thrust geostationary orbit insertion for total ionizing dose decrease. *Cosmic Res.* **57**, 289–300 (2019)
 7. Bizouard, C., Remus, F., Lambert, S., Seoane, L., Gambis, D.: The Earth's variable Chandler wobble. *Astron. Astrophys.* **526**, A106.1–A106.4 (2011)
 8. Munk, W.H., MacDonald, G.J.F.: *The rotation of the Earth*. Cambridge University Press, New York (1961)
 9. Markov, Y.G., Perepelkin, V.V., Filippova, A.S.: Analysis of the perturbed Chandler wobble of the Earth pole. *Dokl. Phys.* **62**(6), 318–322 (2017)
 10. Krylov, S.S., Perepelkin, V.V., Filippova, A.S.: Long-period lunar perturbations in Earth pole oscillatory process: Theory and observations. In: Jain, L.C., Favorskaya, M.N., Nikitin, I.S., Reviznikov, D.L. (eds.) *Advances in Theory and Practice of Computational Mechanics*. SIST, vol. 173, pp. 315–331. Springer, Singapore (2020)
 11. Zlenko, A.A.: A celestial-mechanical model for the tidal evolution of the Earth-Moon system treated as a double planet *Astron. Rep.* **59**(1), 72–87 (2015)
 12. Zlenko, A.A.: The perturbing potential and the torques in one three-body problem. *J. Phys. Conf. Ser.* **1301**, 012022.1–012022.12 (2019)
 13. Akulenko, L.D., Markov, Y.G., Rykhlova, L.V.: Motion of the Earth's poles under the action of gravitational tides in the deformable-Earth model. *Dokl. Phys.* **46**(4), 261–263 (2001)
 14. Information System and Data Center for geoscientific data, <https://isdc.gfz-potsdam.de>, last accessed 2020/09/09.
 15. Guochang, Xu.: *Sciences of Geodesy—I: Advances and Future Directions*. Springer, Berlin, Heidelberg (2010)
 16. Schubert, G.: *Treatise on Geophysics*, vol. 3. Elsevier, Geodesy (2007)
 17. Kumakshev, S.A.: Gravitational-tidal model of oscillations of Earth's poles. *Mech. Solids* **53**(2), 159–163 (2018)
 18. Kumakshev, S.A.: Model of oscillations of Earth's poles based on gravitational tides. In: Karev, V., Klimov, D., Pokazeev, K. (eds.) *Physical and Mathematical Modeling of Earth and Environment Processes*. PMMEEP, 157–163 (2017)
 19. Cowan, N.B., Agol, E., Meadows, V.S., Robinson, T., Livengood, T.A., Deming, D., Lisse, C.M., A'Hearn, M.F., Wellnitz, D.D., Seager, S., Charbonneau, D.: Alien maps of an ocean-bearing world. *Astrophys. J.* **700**(2), 915–923 (2009)
 20. Sidorenkov, N.S.: *The interaction between Earth's rotation and geophysical processes*. Wiley-VCH Verlag GmbH and Co, KGaA (2009)
 21. Sidorenkov, N.S.: Synchronization of terrestrial processes with frequencies of the Earth–Moon–Sun system. *AApTr* **30**(2), 249–260 (2017)
 22. Sidorenkov, N.S.: The Chandler wobble of the poles and its amplitude. In: *Proceedings of the "Journées 2014 Systemes de reference spatio-temporels"*, Pulkovo observatory, Russia, pp. 195–197 (2014)
 23. Sidorenkov, N.S.: Celestial mechanical causes of weather and climate change. *Izv. Atmos. Ocean. Phys.* **52**, 667–682 (2016)
 24. Smart, W.M.: *Celestial Mechanics*. Longmans, Green (1953)
 25. Perepelkin, V.V., Rykhlova, L.V., Filippova, A.S.: Long-period variations in oscillations of the Earth's pole due to lunar perturbations. *Astron. Rep.* **63**(3), 238–247 (2019)